

A SOLAR FLARE MODEL BASED ON MAGNETIC RECONNECTION BETWEEN CURRENT-CARRYING LOOPS

D. B. MELROSE

Special Research Centre for Theoretical Astrophysics, School of Physics, University of Sydney, NSW 2006, Australia

Received 1997 February 19; accepted 1997 April 3

ABSTRACT

A model for solar flares is proposed in which the flare energy is the magnetic energy released when two current-carrying flux loops reconnect to form two new current-carrying flux loops between the original four footpoints. It is assumed that a magnetic flux, $\Delta\Psi$, and an electric current, ΔI , are transferred during the reconnection, subject to the constraint that the flux and the current at each footpoint are unchanged. The change in the magnetic energy is separated into parts due to the transfer of current and of “potential” field, and the latter is neglected (although the argument for doing so is a weak one). The current transferred, ΔI , is assumed equal to its maximum possible value, which is the weaker of the two currents in the initial flux loops. The change in magnetic energy is calculated for some specific simple configurations of the spots (footpoints of the loops). Some favorable configurations for energy release are when a positive polarity spot is near a negative polarity spot (so that one of the final loops is very small) and when the two initial loops are at a large angle to each other. The model allows reconnection only between loops with the same handedness (the sign of the helicity $\propto I/\Psi$) and the handedness is preserved during reconnection. Observational evidence that there is a preferred handedness for coronal magnetic structures suggests that this requirement of the model is automatically satisfied, but specific data on the helicity in active regions is less conclusive. It is energetically favorable for overlapping colinear loops to reconnect to form a longer and a shorter (nested) loop, and it is suggested that very long loops connecting different active regions form through a sequence of such reconnections involving ephemeral flux loops that emerge between the active regions.

Subject headings: MHD — Sun: flares — Sun: magnetic fields

1. INTRODUCTION

An important class of solar flares is known to be associated with the emergence of new magnetic flux in an existing complex active region (e.g., Švestka 1976; Heyvaerts, Priest, & Rust 1977), especially in δ regions in which the polarity of the newly emerging flux is opposite to that of the existing flux (e.g., Zirin & Liggett 1987). The standard interpretation is that magnetic reconnection occurs, releasing magnetic energy to produce the flare. Until quite recently the observational evidence for the implied change in the magnetic topology in the overlying corona was weak. However, recent developments of a technique due originally to Sweet (1958) has allowed the topology of the coronal magnetic field above a sunspot group with four components protruding through the photosphere to be explored. Sweet (1958) found that the overlying structure separates into four regions, determined by the connection of the field lines to the spots, which are identified as the footpoints of magnetic loops. This method was developed further by Baum & Bratenahl (1980), Machado et al. (1988) and Gorbachev & Somov (1988), and recently by Longcope (1996), who referred to the method as magnetic charge topology (MCT). Application of MCT to observational data on solar flares (e.g., Gorbachev & Somov 1989; Mandrini et al. 1991, 1993, 1995; Démoulin et al. 1993, 1994, 1997; Van Driel-Gesztelyi et al. 1994; Bagalá et al. 1995) has shown that the locations of the separatrices between the four regions correlate with flare activity. Brown et al. (1994) summarized the results of the MCT modeling by stating that it supports the suggestions (i) that flare kernels correlate with the intersection of the separatrices with the photosphere, (ii) that the magnetic energy release is associated with currents flowing near the separatrices, and (iii) that changes in the connectivity of the

magnetic field are associated with large flares. Specific changes in magnetic connectivity between different sunspots as the result of large flares have been identified by several groups, e.g., Zirin & Liggett (1987), and Wang, Xu, & Zhang (1994).

There is strong evidence that large-scale currents play a central role in the energy release in solar flares. Recent discussions of relevant data on the currents in coronal loops include those by Gary & Démoulin (1995), Wang et al. (1994), and Leka et al. (1996). In particular, Leka et al. (1996) reported observations of five well observed emerging bipoles and found that the flux bundles that make up these new bipoles are twisted before they emerge and that the new bipoles are cospatial with significant vertical currents. Reconnection between such bipoles occurs when they come into contact in some manner (e.g., Machado et al. 1988), and recent observational evidence for a rapid rise of flux loops in active regions (Uchida et al. 1992) suggests that they are pushed together primarily by this vertical motion rather than by motion of the footpoints. These recent data provide further support for the suggestions (1) that the large-scale currents flow up at one footpoint and down at the other footpoint of a current-carrying loop (Melrose 1991), (2) that the energy released in solar flares is already stored in the current system before the magnetic structures emerge from below the photosphere, and (3) that photospheric motions play no important role in the energetics of solar flares.

Most theories for the energy release in flares are based on reconnection and make no direct reference to the large-scale current. The only standard flare model that takes the current into account directly is that of Alfvén & Carlqvist (1967), but this model is seriously flawed. A central assumption of the model is that magnetic energy is released as the

current decays (due to a postulated formation of a double layer), but the timescale for a flare is much shorter than the time required (the Alfvén propagation time) to affect the source of the current deep in the solar atmosphere. Hence, no significant decay of the current can occur during a flare. The current system can change in the corona during a flare only through a redistribution of current paths, with the net current flowing into and out of the corona at the footpoints remaining fixed. Existing theories do not incorporate the important constraint that the current at each footpoint cannot change significantly during a flare (e.g., Melrose 1992).

In the present paper a model is proposed for estimating the magnetic energy release that results from reconnection between current-carrying magnetic flux loops. As in the model of Sweet (1958), it is assumed that the magnetic flux, Ψ , emerges from below the photosphere in two (positive polarity) spots and submerges at two other (negative polarity) spots. Here Ψ is referred to as the “potential” field, by which is meant only that it is not generated by the large-scale currents that flow into and out of the corona. These spots are the footpoints of flux loops connecting them. Initially, there are two loops connecting the footpoints in pairs. Here the initial loops are denoted loop 1, connecting spots 1+ and 1−, and loop 2, connecting spots 2+ and 2−. The additional assumption is made here that a current, I , is associated with the flux, Ψ , at each spot. A reconnection is defined as a transfer of flux, $\Delta\Psi$, and current, ΔI , between two pairs of loops. This forms loop 3, connecting spots 1+ and 2−, and loop 4, connecting spots 2+ and 1−. This transfer is constrained by the requirement that the flux and current at each footpoint remain fixed.

In order to calculate the change in magnetic energy in the corona due to such a reconnection, simplifying assumptions concerning the geometric configuration of the magnetic fields need to be made. Here, each loop is modeled as a semi-torus with its center and axis in the photosphere. These semi-tori act as “shells” of loops that may correspond to actual loops or to hypothetical (empty) loops. A reconnection transfers flux, $\Delta\Psi$, and current, ΔI , from one loop to another without changing the shape of either. This assumption implies that the calculation of the energy stored in the magnetic field can be separated into a calculation of various coefficients (notably inductances) that depends only

on the assumed geometry (tori of different sizes, displacements, and orientations), which does not change during reconnection. These coefficients are used to determine the energy in terms of Ψ and I , which do change during a reconnection. It is assumed that the favorable conditions for a flare are when (1) the magnetic energy stored in the current system before reconnection is much larger than that after reconnection, and (2) the flux loops in which this energy is stored touch each other so that reconnection becomes possible.

The change in the magnetic energy in the corona is estimated in § 2. The inductances are evaluated for several different specific configurations of the spots in § 3. Application of the model to specific orientations of the spots is discussed in § 4. A particular requirement of the model is that the reconnecting structures have the same handedness or helicity, determined by the sign of I/Ψ , and the observational evidence for this is discussed in § 5. The conclusions are summarized in § 6.

2. THE CHANGE IN MAGNETIC ENERGY

A general form of the model explored here consists of a number of magnetic loops subject to magnetic reconnection. Each loop is defined by its footpoints, magnetic flux and axial current. Let there be N footpoints of positive polarity, denoted $n+$ with $n = 1, \dots, N$, and N footpoints of negative polarity, denoted $n-$. There can be up to N^2 loops connecting the footpoints. The magnetic flux is $\Psi_n > 0$ at $n+$ and $-\Psi_n$ at $n-$, and the current is I_n at $n+$ and $-I_n$ at $n-$. A reconnection involves transfer of flux and current from one pair of initial loops to one pair of final loops. Only the case $N = 2$ is considered in detail here; moreover, only two of the four possible loops (loops 1 and 2) are assumed to be present in the initial state, which is equivalent to the other two (loops 3 and 4) being empty shells, in that initially they have zero flux and current.

2.1. The Constraint on the Current

Suppose that magnetic reconnection occurs between the two flux loops, as illustrated in Figure 1. The four flux loops, labeled 1, 2, 3, and 4, connect the footpoints in pairs (1+, 1−), (2+, 2−), (1+, 2−), and (2+, 1−), respectively. Flux and current are assumed to be transferred together, with the final values denoted by primes. Conservation of

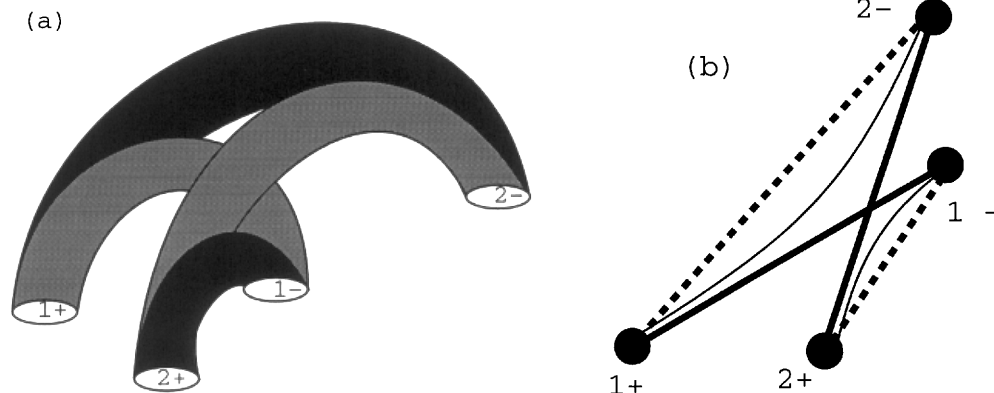


FIG. 1.—Schematic diagram (a) showing initial loops 1 and 2 (lightly shaded) connecting footpoints 1+, 1− and 2+, 2−, respectively, and final loops 3 and 4 (darkly shaded) connecting footpoints 1+, 2− and 2+, 1−, respectively; and (b) showing how the loops reconnect when viewed from above, with heavy solid lines denoting initial loops, heavy dashed lines showing final loops, and light lines indicating a field/current lines in the process of transferring from the initial to the final loops.

current at the footpoints 1+, 2+, 1-, and 2- requires

$$\begin{aligned} I_1 + I_3 &= I'_1 + I'_3, & I_2 + I_4 &= I'_2 + I'_4, \\ I_1 + I_4 &= I'_1 + I'_4, & I_2 + I_3 &= I'_2 + I'_3, \end{aligned} \quad (1)$$

respectively. It follows that one has

$$I_1 - I'_1 = I_2 - I'_2 = \Delta I, \quad I_3 - I'_3 = I_4 - I'_4 = -\Delta I, \quad (2)$$

where ΔI is an undetermined constant, identified as the current transferred in the reconnection. An analogous discussion of the fluxes, which follows by replacing I by Ψ in the foregoing, implies an analogous flux transfer, $\Delta\Psi$.

Let the *handedness* of a particular loop be defined as the sign of the ratio I/Ψ of that loop. (The magnetic helicity, referred to here simply as the helicity, is also determined by I/Ψ .) Thus, loop 1 is right hand (RH) if the current is up ($I_1 > 0$) at 1+ and down at 1-, and it is left hand (LH) in the opposite case ($I_1 < 0$). The handedness so defined corresponds to the sense of twist of the magnetic field.

There is an important implication that follows from the basic requirements of this model if one makes the additional plausible assumption that the current in neither initial flux loop can increase in magnitude as a result of the reconnection. Suppose that loop 1 is RH; this assumption then implies that ΔI is positive, in order that I'_1 be less than I_1 . It follows from $I'_3 = \Delta I$ and $\Psi'_3 = \Delta\Psi$ that loop 3 is also RH. Moreover, equation (2) with $I_1 \geq \Delta I$ requires $I_2 \geq \Delta I$, so that loop 2 must also be RH. Similarly, loop 4 must be RH. Thus, reconnection can occur only between flux loops that have the handedness. Moreover, the maximum current that can be transferred from one footpoint to the other is the minimum of I_1 and I_2 . In particular if one of the initial flux loops carries no current, then it is not possible for the reconnection, as defined here, to occur. (This conclusion follows from the assumption that current and magnetic flux are transferred together, so that reconnection with zero transfer of current is possible only if both initial flux loops have zero current.)

2.2. The Change in the Magnetic Energy Due to the Currents

The magnetic energy associated with the system of currents in the initial (i) and final (f) flux loops may be written in the general form:

$$E_i^1 = \sum_{n,m} M_{nm} I_n I_m, \quad E_f^1 = \sum_{n,m} M_{nm} I'_n I'_m, \quad (3)$$

respectively, where $L_n = M_{nn}$ is the self-inductance of flux loop n , and $M_{mn} = M_{nm}$ for $m \neq n$ is the mutual inductance between flux loops n and m . As explained above, in the present model it is assumed that the reconnection does not affect the shape of the loops, which are thought of as the shells of loops that may or may not be actual loops. For example, if loops 3 and 4 do not exist initially, then in the expression (3) for E_i^1 one has $I_3 = 0$ and $I_4 = 0$, but the coefficients M_{nm} involving $n = 3$ or $m = 3$ are assumed to be well defined and not to change between the initial and the final states. This assumption should not lead to significant error because it is well known that the self-inductance is sensitive only to the length of the current path and is only a weak function of the current profile, and that the mutual inductance is sensitive to the length, separation and orientation of the two current segments, but not to the current profile within each segment.

The energy released is the difference between the initial and final magnetic energies. Only the case of two initial pairs of spots is considered here. Throughout most of this paper it is assumed (1) that loops 1 and 2 are the initial loops, (2) that loops 3 and 4 are formed as a result of reconnection, and (3) that the maximum amount of flux and current is transferred so that either loop 1 or loop 2 disappears as a result of the reconnection. However, before specializing to this case, it is relevant for a later purpose to formulate the problem more generally by assuming that loops 3 and 4 have nonzero initial currents, I_{3i} and I_{4i} , respectively, and that loops 1 and 2 have nonzero final currents, I_{1f} and I_{2f} , respectively. Then one has $I_1 = I_{1f} + \Delta I$, $I_2 = I_{2f} + \Delta I$, $I'_1 = I_{1f}$, $I'_2 = I_{2f}$, and $I_3 = I_{3i}$, $I_4 = I_{4i}$, $I'_3 = I_{3i} + \Delta I$, $I'_4 = I_{4i} + \Delta I$. The transfer of current ΔI leads to a change in energy

$$\Delta E^1 = R \Delta I + M^{\text{IR}} (\Delta I)^2, \quad (4)$$

$$R = M_1^{\text{LCS}} I_{1f} + M_2^{\text{LCS}} I_{2f} - M_3^{\text{LCS}} I_{3i} - M_4^{\text{LCS}} I_{4i}, \quad (5)$$

$$M_n^{\text{LCS}} = M_{n1} + M_{n2} - M_{n3} - M_{n4}, \quad (6)$$

$$M^{\text{IR}} = \frac{1}{2}(L_1 + L_2 - L_3 - L_4) + M_{12} - M_{34}. \quad (7)$$

Magnetic energy is released, implying that the reconnection can occur spontaneously, for $\Delta E^1 > 0$.

The change in magnetic energy is separated into two terms on the right-hand side of equation (4). The first term is referred to as the *irreducible reconnection* (IR) term. One may interpret the IR term in equation (4) as follows: separate the currents into the parts that do not change and the parts that are transferred in the reconnection; the IR term is the energy change when only the latter parts of the currents are retained. The IR term corresponds to $I_{1f} = I_{2f} = I_{3i} = I_{4i} = 0$, so that one has $I_1 = I_2 = \Delta I$ initially and $I_3 = I_4 = \Delta I$ finally, with all other currents zero. The other term in equation (4) may be attributed to an additional contribution from the magnetic energy released when like currents separate, and this term is referred to as the *like current separation* (LCS) term. The LCS term takes account of the change due to the effective mutual inductance as currents move apart or together. Consider the specific case $I_{1f} = I_1 - I_2$, $I_{2f} = I_{3i} = I_{4i} = 0$, and hence $\Delta I = I_2$. Then only the term involving M_1^{LCS} contributes in the LCS term (eq. [5]). One can interpret the four terms in equation (6), specifically $M_1^{\text{LCS}} = L_1 + M_{12} - M_{13} - M_{14}$, as follows. The initial magnetic energy associated with the current in loop 1 is $\frac{1}{2}L_1 I_1^2 = \frac{1}{2}L_1 I_{1f}^2 + \frac{1}{2}L_1 (\Delta I)^2 + L_1 I_{1f} \Delta I$. The first term is unaffected by the reconnection, the second term contributes to the IR term in equation (4) and the third term gives the L_1 term in M_1^{LCS} . In this context, L_1 may be interpreted as the initial mutual inductance between the two parts I_{1f} , ΔI of the initial current. Thus, the term L_1 in M_1^{LCS} may be interpreted in terms of the change in the magnetic energy as these two parts of the initial current move apart. The next term, M_{12} in M_1^{LCS} , arises from the magnetic energy associated with the mutual inductance between I_{1f} and $I_2 = \Delta I$ in the initial state. The final two terms arise from the magnetic energy associated with the mutual inductance between I_{1f} and $I_3 = \Delta I$ and $I_4 = \Delta I$, respectively, in the final state. Thus, the LCS terms take into account the net effect of the energy change as the various parts of the current move apart or together.

2.3. Specific Model for the Change in Magnetic Energy

In the following discussion, loop 1 is assumed longer than loop 2 ($a_1 > a_2$), and the maximum possible current is assumed to be transferred in the reconnection. Hence, the change in the magnetic energy is given by

$$\Delta E^I = \begin{cases} M_1^{\text{LCS}}(I_1 - I_2)I_2 + M^{\text{IR}}I_2^2 & \text{for } I_1 > I_2, \\ M_2^{\text{LCS}}(I_2 - I_1)I_1 + M^{\text{IR}}I_1^2 & \text{for } I_2 > I_1, \end{cases} \quad (8)$$

which follows from equation (4) for $I_3 = I_4 = 0$ and $\Delta I = |I_1 - I_2|$. The coefficients in equation (8) are given by equations (6) and (7), respectively.

2.4. Flux Loops as Half-Tori

In the idealized model for the reconnecting magnetic structures adopted here the flux loops above the photosphere are modeled as the visible halves of tori whose axes of symmetry are in the photosphere, as illustrated in Figure 2. Let the n th torus have a major radius a_n , a cross-sectional area $A_n = \pi r_n^2$, where r_n is the minor radius, and have its axis of symmetry along the direction defined by the unit vector \mathbf{n}_n . The self-inductance, L_n , of the n th loop is (e.g., Landau & Lifshitz 1960, p. 139),

$$L_n = \mu_0 C a_n, \quad C = \left(\ln \frac{8a_n}{r_n} - \frac{7}{4} \right), \quad (9)$$

where the term $7/4$ applies for a uniform current profile; other profiles are discussed by Book, Turchi, & Stein (1979). One has $C = 0.7$ for $a_n/r_n = 3$ and $C = 1.3$ for $a_n/r_n = 10$.

We also require an appropriate expression for the mutual induction, M_{nm} , of two loops. Specifically, consider two loops with major radii a_n, a_m , whose centers are separated by a distance d_{nm} , and which are oriented at an angle $\theta_{nm} = \arccos(\mathbf{n}_n \cdot \mathbf{n}_m)$. A suitable approximation for the mutual inductances needs to satisfy the requirement $M_{nm} = (L_n L_m)^{1/2}$ for $a_n = a_m, d_{nm} = 0$ and $\theta_{nm} = 0$. The following form is an interpolation between some known results summarized in the Appendix and the requirement $M_{nm} = (L_n L_m)^{1/2}$ for identical, parallel, coincident loops:

$$M_{nm} = \mu_0 C \frac{8a_n^2 a_m^2 \cos \theta_{nm}}{[(a_n + a_m)^2 + d_{nm}^2]^{3/2}}. \quad (10)$$

The actual values of the mutual inductances play an important role in the model, as developed below, and the numerical results rely on the form of equation (10). It should be emphasized that equation (10) is an interpolation between known results, which are themselves derived under idealized conditions.

2.5. The Change Due to the "Potential" Field

The energy in the "potential" field, described by the magnetic fluxes, may also change as a result of reconnection. A semiquantitative estimate of the magnetic energy in a flux loop with a magnetic flux Ψ_n follows by noting that if the flux loop were a cylinder of length $\ell_n = \pi a_n$ and area A_n with an axial magnetic field B_n , then one has $\Psi_n = B_n A_n$ and a magnetic energy $B_n^2 \ell_n A_n / 2\mu_0$. In the model considered here, the flux loop is a semi-torus, but in practice, the cross section of a coronal flux loop may vary between its footpoints and its top. To take this possibility into account a factor, β , of order unity is included in identifying the

magnetic energy as $\beta \pi a_n \Psi_n^2 / \mu_0 A_n$, where A_n is the average cross section along the length of the loop.

The change in the "potential" energy, analogous to the change (eq. [8]) in the energy associated with the currents, then reduces to

$$\Delta E^P = \beta \pi \left(\frac{a_1}{A_1} + \frac{a_2}{A_2} - \frac{a_3}{A_3} - \frac{a_4}{A_4} \right) \frac{(\Delta \Psi)^2}{\mu_0} + \begin{cases} \frac{\beta \pi a_1}{A_1} 2(\Psi_1 - \Psi_2) \Delta \Psi & \text{for } \Psi_1 > \Psi_2 = \Delta \Psi, \\ \frac{\beta \pi a_2}{A_2} 2(\Psi_2 - \Psi_1) \Delta \Psi & \text{for } \Psi_2 > \Psi_1 = \Delta \Psi. \end{cases} \quad (11)$$

The first term on the right-hand side of equation (11) is the analog of the IR term in equation (8). Whether this term is positive or negative depends on how the cross section, A_n , scales with length, πa_n , of a typical flux loop during the reconnection process. The final term on the right-hand side of equation (11) is always positive. Let us consider these two terms separately.

Suppose one assumes that the scaling during reconnection is $A_n \propto a_n^\zeta$, so that the mean magnetic field along the flux loop is $\propto a_n^{-\zeta}$, where a_n may be reinterpreted as the height of the top of the flux loop above the photosphere. For example, consider a dipolar model in which the flux loop is assumed to have a dipolar shape, say with the dipole a depth h_n below the photosphere; then the magnetic field at the top of the loop scales $\propto (h_n + a_n)^{-3}$. This suggests $1 \lesssim \zeta \lesssim 3$ as a plausible range for the scaling. For $\zeta \approx 1$ the first term on right-hand side of equation (11) is close to zero, and for $\zeta > 1$ it tends to be negative if one of the new loops is much shorter than the two initial loops. Whether the expected negative contribution from this term is larger or smaller than the positive contribution from the final term in equation (11) is uncertain, due both to its dependence on this uncertain scaling and to its dependence on the values of Ψ_1 and Ψ_2 .

The final term in equation (11), say for $\Psi_1 > \Psi_2$, is analogous to the LCS term in equation (8), and one can compare the magnitude of these changes in the "potential" and current-induced terms given for a given value of the ratio $\Delta I / \Delta \Psi$. Suppose one assumes that there is a characteristic helicity, described by a characteristic value of I / Ψ (cf. § 5), and that the reconnection maintains this value, implying $\Delta I / \Delta \Psi = I_1 / \Psi_1 = I / \Psi$. Then the ratio of the LCS term in equation (8) to the final term in equation (11) is $(\mu_0 A_1 M_1^{\text{LCS}} / 2\pi \beta a_1) (I / \Psi)^2$. The angle of twist, ϕ , of a flux loop is

$$\tan \phi = \left(\frac{B_\phi}{B_z} \right) = \frac{\mu_0 R I}{2\Psi}, \quad (12)$$

with $R = (A_1 / \pi)^{1/2}$ here. Writing $M_1^{\text{LCS}} = \mu_0 \Delta a_1$, the ratio of these two terms reduces to $(2\Delta a_1 / a_1) \tan^2 \phi_1$, where ϕ_1 is the angle of twist at the top of the flux loop. For a loop whose cross section at its top is much larger than at its footpoint, the twist at the top of the loop is much larger than at the footpoint ($\tan \phi \propto A^{1/2}$). If such a loop were moderately twisted at its footpoint, it would be strongly twisted near its top, implying $\tan^2 \phi_1 > 1$ under plausible conditions. In such a situation, the ratio of the LCS term in equation (8) to the final term in equation (11) would be $(2\Delta a_1 / a_1) \tan^2 \phi_1$, and the change (eq. [11]) could justifiably be ignored in comparison to equation (8).

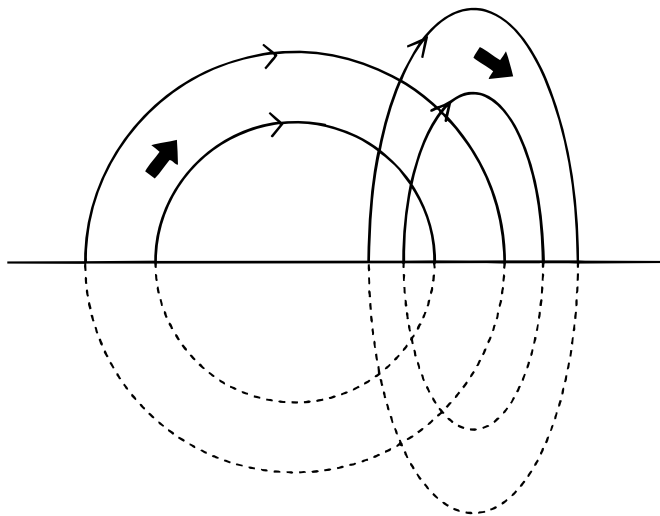


FIG. 2.—Schematic diagram indicating the model of loops as semi-tori, with each torus projected as a ring; the regions below the photosphere are shown dashes, and the light arrows indicate the direction of the magnetic field and the solid arrows indicate the direction of the current.

The foregoing arguments suggest that one may be justified in neglecting the change (eq. [11]) in the energy associated with the “potential” field in comparison with the change (eq. [8]) in the magnetic energy associated with the large-scale current system. Here the change (eq. [11]) is ignored, and although this assumption is discussed further in § 4, the justification for it remains relatively weak. An entirely different model based on the change (eq. [11]) in the magnetic energy could be formulated, but this is not attempted here.

3. APPLICATION TO SPECIFIC MAGNETIC CONFIGURATIONS

In this section the energy change (eq. [8]) is considered as a function of the relative locations of the various footpoints for a few idealized configurations. The objective is to identify the cases for which the largest fraction of the stored magnetic energy is released.

3.1. A Four Spot Model

Suppose that the four spots, identified as the footpoints of flux loops, are at positions $x_{n\pm}, y_{n\pm}$, with $n = 1, 2$. The radius of the n th loop is then

$$a_n = \frac{1}{2}[(x_{n+} - x_{n-})^2 + (y_{n+} - y_{n-})^2]^{1/2}, \quad (13)$$

the distance, d_{nm} , between the centers of loops n and m is

$$d_{nm} = \frac{1}{2}[(x_{n+} + x_{n-} - x_{m+} - x_{m-})^2 + (y_{n+} + y_{n-} - y_{m+} - y_{m-})^2]^{1/2}, \quad (14)$$

and the angle between the normal loops n and m may be written as $\theta_{nm} = \theta_n - \theta_m$ with

$$\theta_n = \arctan \frac{y_{n+} - y_{n-}}{x_{n+} - x_{n-}}. \quad (15)$$

These values are to be inserted in the expressions (6) and (7) for the coefficients in equation (8).

3.2. Particular Configurations

The general model, described by equations (13), (14), and (15), involves five free parameters, one of which is a scaling parameter and the other four define the shape. Specific simplifying assumptions are needed to reduce this to a manageable number of free parameters. To identify some favorable and unfavorable possibilities, consider the following specific configurations.

Case 1a: Collinear spots, normal polarity.—First, suppose that all four spots are on the same line, along the x -axis. Also suppose that both initial loops have “normal” polarity, defined such that $n+$ is to the left of $n-$. As the labelings are arbitrary, we are free to choose the leftmost spot to be $1+$ and loop 1 to be the larger ($a_1 \geq a_2$). There are then only two relevant different configurations: $1+, 2+, 1-, 2-$ (overlapping loops) and $1+, 2+, 2-, 1-$ (nested loops). (According to the model reconnection is not possible for $1+, 1-, 2+, 2-$, which corresponds to disjoint loops.) A reconnection converts overlapping loops into nested loops, or nested loops into overlapping loops. In exploring which reconnection is energetically favorable, only one configuration needs to be considered, and that with overlapping loops is chosen. The configuration is then as illustrated in Figure 3a.

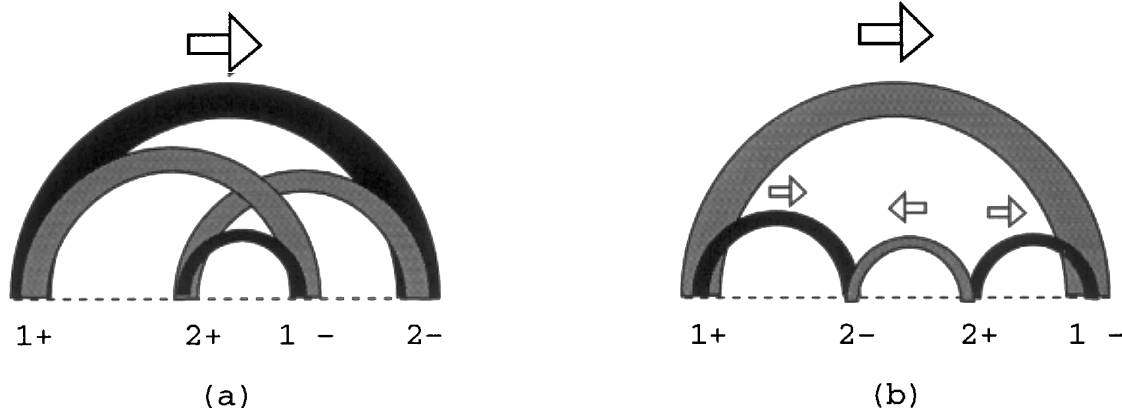


FIG. 3.—Reconnection between two collinear loops, with the initial loops shown lightly shaded and the final loops shown darkly shaded and with the arrows indicating the direction of the currents: (a) initially overlapping loops with the same polarity reconnect into a longer loop and a shorter nested loop; (b) nested loops of opposite polarity reconnect into disjoint loops whose net length is shorter than the net length of the initial loops.

This model involves three free parameters, which are chosen to be a_1 , a_2 and the distance between the centers of the initial loops, $d_{12} = d$. Overlapping loops require $a_1 - a_2 \leq d \leq a_1 + a_2$. In this configuration one has

$$\begin{aligned} a_3 &= \frac{1}{2}(a_1 + a_2 + d), \quad a_4 = \frac{1}{2}(a_1 + a_2 - d), \quad d_{12} = d, \\ d_{13} &= a_3 - a_1, \quad d_{14} = a_1 - a_4, \quad d_{23} = a_3 - a_2, \\ d_{24} &= a_2 - a_4, \quad d_{34} = a_1 - a_2, \end{aligned} \tag{16}$$

with $\cos \theta_{nm} = 1$ for all loops. Then the coefficients in equation (8) may be written in the form

$$\begin{aligned} M_1^{\text{LCS}} &= \mu_0 C \left[a_1 + \frac{8a_1^2 a_2^2}{[(a_1 + a_2)^2 + d^2]^{3/2}} \right. \\ &\quad \left. - \frac{\sqrt{8a_1^2 a_3^2}}{(a_1^2 + a_3^2)^{3/2}} - \frac{\sqrt{8a_1^2 a_4^2}}{(a_1^2 + a_4^2)^{3/2}} \right], \\ M_2^{\text{LCS}} &= \mu_0 C \left[a_2 + \frac{8a_1^2 a_2^2}{[(a_1 + a_2)^2 + d^2]^{3/2}} \right. \\ &\quad \left. - \frac{\sqrt{8a_2^2 a_3^2}}{(a_2^2 + a_3^2)^{3/2}} - \frac{\sqrt{8a_2^2 a_4^2}}{(a_2^2 + a_4^2)^{3/2}} \right], \\ M^{\text{IR}} &= \mu_0 C \left[\frac{8a_1^2 a_2^2}{[(a_1 + a_2)^2 + d^2]^{3/2}} - \frac{\sqrt{8a_3^2 a_4^2}}{(a_1^2 + a_2^2)^{3/2}} \right], \end{aligned} \tag{17}$$

with $a_3 > a_1 > a_2 > a_4$, $a_1 + a_2 = a_3 + a_4$. The coefficients vanish for $d = a_1 - a_2$, when one has $a_3 = a_1$, $a_4 = a_2$, and the reconnection does not change the configuration. As $d > a_1 - a_2$ increases, a_3 increases and a_4 decreases, and the coefficients (eq. [17]) all increase. In the limiting case $d = a_1 + a_2$, when spots 1- and 2+ coincide, loop 4 is negligible, $a_4 = 0$, and the energy change is maximized. The limit $a_4 = 0$ is discussed more generally as case 2 below.

Case 1b: Collinear spots, reverse polarity.—Next suppose that the two initial loops are collinear with opposite polarities, as illustrated in Figure 3b. Unlike case 1a, the two configurations of nested and overlapping loops do not interchange as a result of reconnection, and both need to be discussed. For either, reconnection leads to two disjoint final loops, with the same polarity for initially nested loops and with opposite polarity for initially overlapping loops.

For nested initial loops one has $a_3 + a_4 = a_1 - a_2$, $d = a_3 - a_4 < a_1 - a_2$ and then the coefficients in equation (8) reduce to

$$\begin{aligned} M_1^{\text{LCS}} &= \mu_0 C \\ &\times \left[a_1 - \frac{8a_1^2 a_2^2}{[(a_1 + a_2)^2 + d^2]^{3/2}} - \frac{\sqrt{8a_1^2 a_3^2}}{(a_1^2 + a_3^2)^{3/2}} - \frac{\sqrt{8a_1^2 a_4^2}}{(a_1^2 + a_4^2)^{3/2}} \right], \\ M_2^{\text{LCS}} &= \mu_0 C \\ &\times \left[a_2 - \frac{8a_1^2 a_2^2}{[(a_1 + a_2)^2 + d^2]^{3/2}} + \frac{\sqrt{8a_2^2 a_3^2}}{(a_2 + a_3)^3} + \frac{\sqrt{8a_2^2 a_4^2}}{(a_2 + a_4)^3} \right], \\ M^{\text{IR}} &= \mu_0 C \left\{ a_2 - \frac{8a_1^2 a_2^2}{[(a_1 + a_2)^2 + d^2]^{3/2}} - \frac{\sqrt{8a_3^2 a_4^2}}{(a_1^2 + a_2^2)^{3/2}} \right\}. \end{aligned} \tag{18}$$

For overlapping loops one has $a_3 - a_4 = a_1 - a_2$, $d = a_3$

+ $a_4 > a_1 - a_2$, and equation (18) is replaced by

$$\begin{aligned} M_1^{\text{LCS}} &= \mu_0 C \\ &\times \left\{ a_1 - \frac{8a_1^2 a_2^2}{[(a_1 + a_2)^2 + d^2]^{3/2}} - \frac{\sqrt{8a_1^2 a_3^2}}{(a_1^2 + a_3^2)^{3/2}} + \frac{\sqrt{8a_1^2 a_4^2}}{(a_1 + a_4)^3} \right\}, \\ M_2^{\text{LCS}} &= \mu_0 C \\ &\times \left\{ a_2 - \frac{8a_1^2 a_2^2}{[(a_1 + a_2)^2 + d^2]^{3/2}} + \frac{\sqrt{8a_2^2 a_3^2}}{(a_2 + a_3)^3} - \frac{\sqrt{8a_1^2 a_4^2}}{(a_1^2 + a_4^2)^{3/2}} \right\}, \\ M^{\text{IR}} &= \mu_0 C \left\{ \frac{1}{2} (a_1 + a_2 - d) - \frac{8(a_1^2 a_2^2 - a_3^2 a_4^2)}{[(a_1 + a_2)^2 + d^2]^{3/2}} \right\}. \end{aligned} \tag{19}$$

The two forms, equations (18) and (19), coincide for $d = a_1 - a_2$, when one has $a_4 = 0$, which is discussed below as a limit of case 2 below. More generally, inspection of the signs of the terms in equations (18) and (19), together with the inequality $a_3 > a_4$, suggests that M_2^{LCS} is the largest of the coefficients provided that a_2/a_1 is not too small. (This is confirmed below for the special case $a_4 = 0$.) This leads to the conclusion that reconnection when the smaller loop has reverse polarity is favorable provided that the smaller loop has the stronger current, that is, for $I_2 > I_1$ in equation (8).

Case 2: Triangular configuration: two coincident spots.—Next suppose that the spots 2+ and 1- coincide, so that the spots form a triangle with sides $2a_1$, $2a_2$, $2a_3$, with $a_4 = 0$, as illustrated in Figure 4. Let the angle between the sides $2a_1$ and $2a_2$ be θ . Then one has

$$\begin{aligned} a_3 &= (a_1^2 + a_2^2 - 2a_1 a_2 \cos \theta)^{1/2}, \\ d_{12} &= a_3, \quad d_{13} = a_2, \quad d_{23} = a_1, \\ \cos \theta_{12} &= -\cos \theta, \quad \cos \theta_{13} = \frac{(a_3^2 - a_2^2 \sin^2 \theta)^{1/2}}{a_3}, \\ \cos \theta_{23} &= \mp \frac{(a_3^2 - a_1^2 \cos^2 \theta)^{1/2}}{a_3}, \end{aligned} \tag{20}$$

with the upper sign for $a_3^2 < a_1^2 - a_2^2 (\cos \theta > a_2/a_1)$ and the lower sign for $a_3^2 > a_1^2 - a_2^2 (\cos \theta < a_2/a_1)$. The coefficients in equation (8) reduce to

$$\begin{aligned} M_1^{\text{LCS}} &= \mu_0 C \\ &\times \left\{ a_1 - \frac{8a_1^2 a_2^2 \cos \theta}{[(a_1 + a_2)^2 + a_3^2]^{3/2}} - \frac{8a_1^2 a_3 (a_3^2 - a_2^2 \sin^2 \theta)^{1/2}}{[(a_1 + a_3)^2 + a_2^2]^{3/2}} \right\}, \\ M_2^{\text{LCS}} &= \mu_0 C \\ &\times \left\{ a_2 - \frac{8a_1^2 a_2^2 \cos \theta}{[(a_1 + a_2)^2 + a_3^2]^{3/2}} \pm \frac{8a_1^2 a_3 (a_3^2 - a_1^2 \sin^2 \theta)^{1/2}}{[(a_2 + a_3)^2 + a_1^2]^{3/2}} \right\}, \\ M^{\text{IR}} &= \mu_0 C \left\{ \frac{1}{2} (a_1 + a_2 - a_3) - \frac{8a_1^2 a_2^2 \cos \theta}{[(a_1 + a_2)^2 + a_3^2]^{3/2}} \right\}, \end{aligned} \tag{21}$$

The expressions reproduces the limit $a_4 = 0$ of case 1a and case 1b (nested loops) for $\cos \theta = -1$ and $\cos \theta = 1$, respectively.

For $\cos \theta = -1$, equation (21) reproduces the limit $a_4 = 0$ in equation (17). For example for initial loops with $a_2 = a_1/2$, equation (21) implies $M_1^{\text{LCS}} = 0.12\mu_0 C a_1$, $M_2^{\text{LCS}} = 0.31\mu_0 C a_1$, $M^{\text{IR}} = 0.21\mu_0 C a_1$, and for $a_2 = a_1$,

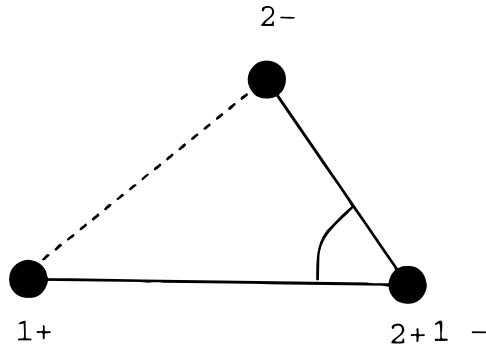


FIG. 4.—Triangular configuration in which spots 1- and 2+ coincide; the initial loops are shown as solid lines, and the final loop as a dashed line.

equation (21) implies $M_1^{LCS} = M_2^{LCS} \approx M^{IR} = 0.35\mu_0 Ca_1$. Reconnection is energetically favorable for initially overlapping loops to form a larger final loop with a smaller nested loops, and these examples correspond to the optimum case when the smaller loop is negligible.

For $\cos \theta = 1$, equation (21) reproduces the limit $a_4 = 0$ in equation (18). For this case, note that equation (21) implies $M_1^{LCS} = M_2^{LCS} = M^{IR} = 0$ for both $a_2 = 0$ (only one loop) and $a_2 = a_1$ (canceling identical loops). Between these limits M_1^{LCS} changes sign three times and M^{IR} once, both being positive for small a_2/a_1 . For $a_2 = a_1/2$ one finds $M_2^{LCS} = 0.17\mu_0 Ca_1 \gg |M_1^{LCS}|, |M^{IR}|$. One concludes that while case 1b with $I_1 > I_2$ and $a_4 = 0$ allows energy release on reconnection for small a_2 , it is not a particularly favorable configuration for energy release. On the other hand, for $I_2 > I_1$, the coefficient M_2^{LCS} is relevant (cf. eq. [8]), and it can be moderately large. It follows that the case where loop 2 has reverse polarity is favorable for energy release on reconnection provided that loop 2 has the larger current.

For orthogonal initial loops, $\cos \theta = 0$ in equation (21) gives moderately large and positive values for the coefficients. For example, for $a_2 = a_1/2$ equation (21) implies $M_1^{LCS} = 0.13\mu_0 Ca_1, M_2^{LCS} = 0.47\mu_0 Ca_1, M^{IR} = 0.19\mu_0 Ca_1$. The coefficients are not strong functions of $\cos \theta$ when $\cos \theta$ is small, so that there is a broad range of both a_2/a_1 and $\cos \theta$, where these positive values apply. One concludes that this is a relatively favorable configuration for

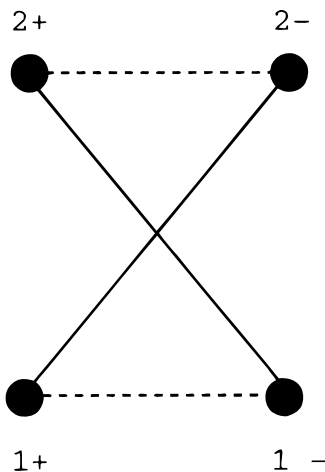


FIG. 5.—Same as in Fig. 4 but for a rectangular configuration of the spots.

a moderately large energy release.

Case 3: Spots forming a rectangle.—In general, the four spots define a quadrilateral. Suppose the spots define the four corners of a rectangle, with sides of length $2a$ and $2b$, as illustrated in Figure 5. The initial loops overlap only if they are along the diagonals of the rectangle, and the final loops are then along two opposing sides of the rectangle. Let the final loops correspond to the sides of length $2a$, so that the initial loops have radii b and the final loops have radii a . Choosing the spots to be at $1+ = \frac{1}{2}(-a, -b), 1- = \frac{1}{2}(a, b), 2+ = \frac{1}{2}(-a, b), 2- = \frac{1}{2}(a, -b)$, one has

$$a_1 = a_2 = \sqrt{a^2 + b^2}, \quad a_3 = a_4 = a, \quad d_{12} = 0, \\ d_{13} = d_{14} = d_{23} = d_{24} = b, \quad d_{34} = 2b, \\ \cos \theta_{12} = \frac{a^2 - b^2}{a^2 + b^2},$$

$$\cos \theta_{13} = \cos \theta_{14} = \cos \theta_{23} = \cos \theta_{24} = \frac{a}{\sqrt{a^2 + b^2}},$$

$$\cos \theta_{34} = 1. \tag{22}$$

The coefficients in equation (8) reduce to

$$M_1^{LCS} = M_2^{LCS} = \mu_0 C \\ \times \left\{ \sqrt{a^2 + b^2} + \frac{a^2 - b^2}{\sqrt{a^2 + b^2}} - \frac{16a^3 \sqrt{a^2 + b^2}}{[(\sqrt{a^2 + b^2} + a)^2 + b^2]^{3/2}} \right\}, \\ M^{IR} = \mu_0 C \left[\sqrt{a^2 + b^2} - a + \frac{a^2 - b^2}{\sqrt{a^2 + b^2}} - \frac{a^4}{(a^2 + b^2)^{3/2}} \right]. \tag{23}$$

The limit $b^2 \gg a^2$ is not favorable because the initial energy in the current system is small (the currents are nearly antiparallel). The limit $b^2 \ll a^2$ is also not favorable because the reconnection then makes only a small change in the current paths.

The optimum case is that of a square ($a = b, a_1 = 2^{1/2}a$), when equation (23) reduces to $M_1^{LCS} = M_2^{LCS} = 0.10\mu_0 Ca_1, M^{IR} = 0.04\mu_0 Ca_1$. Thus, the coefficients in equation (8) are positive, suggesting that the configuration is favorable for energy release. However, the magnitudes of the coefficients are not as large as in the triangular configuration.

Case 4: Orthogonal final loops.—As a final example, consider a configuration suggested by reconnecting flaring loops identified recently by Nishio et al. (1997) from X-ray and microwave data. Figure 6 is a cartoon of the active region. An idealized configuration for this case corresponds to three of the spots in a line and the final two loops orthogonal, as illustrated in Figure 7, specifically with the following locations for the spots: $1+ = (-2a_1, 0), 1- = (0, 0), 2+ = (0, 2a_2 \sin \theta), 2- = (-2a_2 \cos \theta, 0)$, with θ the acute angle between loops 1 and 2. Then one has

$$a_3 = a_1 - a_2 \cos \theta, \quad a_4 = a_2 \sin \theta,$$

$$d_{12}^2 = d_{34}^2 = a_1^2 + a_2^2 - 2a_1 a_2 \cos \theta,$$

$$d_{13}^2 = d_{23}^2 = a_2^2 \cos^2 \theta,$$

$$d_{24}^2 = a_2^2, \quad d_{34}^2 = a_1^2 + a_2^2 + 2a_1 a_2 \cos \theta,$$

$$\cos \theta_{12} = \cos \theta_{23} = -\cos \theta, \quad \cos \theta_{24} = \sin \theta, \tag{24}$$

with $\cos \theta_{13} = 1, \cos \theta_{14} = 0$. The coefficients in equation

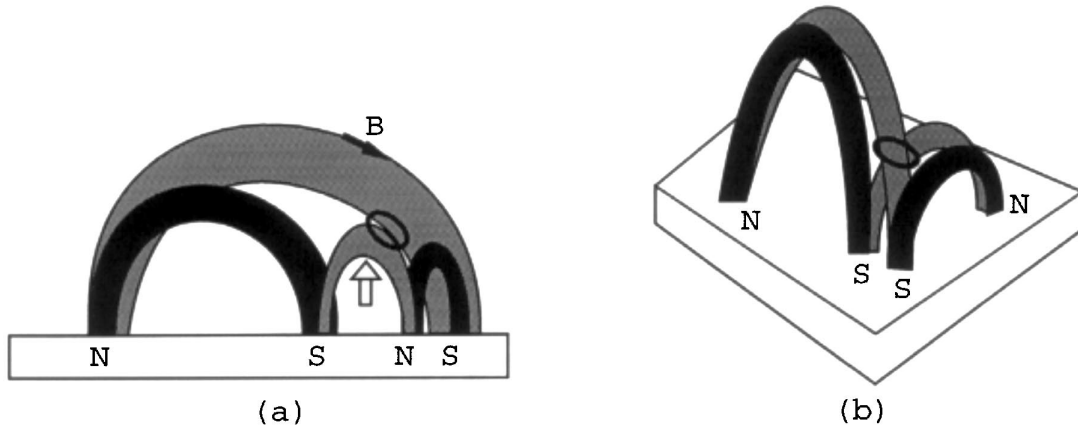


FIG. 6.—Idealized model for reconnecting loops based on a specific event discussed by Nishio et al. (1997); (a) the light arrow indicates the rising motion of the emerging flux loop, the solid arrows indicate the direction of the magnetic field, and the ring indicates the reconnection region; (b) same as for (a) viewed from a different angle.

(8) reduce to

$$M_1^{LCS} = \mu_0 C \left\{ a_1 - \frac{\sqrt{8a_1^2 a_2^2 \cos \theta}}{[a_1^2 + a_2^2 + a_1 a_2(1 - \cos \theta)]^{3/2}} - \frac{\sqrt{8a_1^2(a_1 - a_2 \cos \theta)^2}}{[2a_1^2 + a_2^2 \cos^2 \theta - 2a_1 a_2 \cos \theta]^{3/2}} \right\},$$

$$M_2^{LCS} = \mu_0 C \left\{ a_2 - \frac{\sqrt{8a_1^2 a_2^2 \cos \theta}}{[a_1^2 + a_2^2 + a_1 a_2(1 - \cos \theta)]^{3/2}} + \frac{\sqrt{8a_2^2(a_1 - a_2 \cos \theta)^2 \cos \theta}}{[a_1^2 + a_2(a_1 + a_2)(1 - \cos \theta)]^{3/2}} - \frac{8a_2 \sin^3 \theta}{(2 + 2 \sin \theta + \sin^2 \theta)^{3/2}} \right\},$$

$$M^{IR} = \mu_0 C \left\{ \frac{1}{2} (a_2(1 + \cos \theta - \sin \theta)) - \frac{\sqrt{8a_1^2 a_2^2 \cos \theta}}{[a_1^2 + a_2^2 + a_1 a_2(1 - \cos \theta)]^{3/2}} \right\}, \quad (25)$$

respectively. On evaluating the coefficients equation (25) for $a_2 = a_1/2$, $\cos \theta = \frac{1}{2}$, one finds $M_1^{LCS} = -0.01\mu_0 C a_1$, $M_2^{LCS} = 0.16\mu_0 C a_1$, $M^{IR} = -0.03\mu_0 C a_1$. It follows that this configuration is moderately favorable for energy release, but only for $I_2 > I_1$.

4. IMPLICATIONS OF THE MODEL

Applications of the foregoing model to solar flares and to the formation of magnetic loops linking active regions are

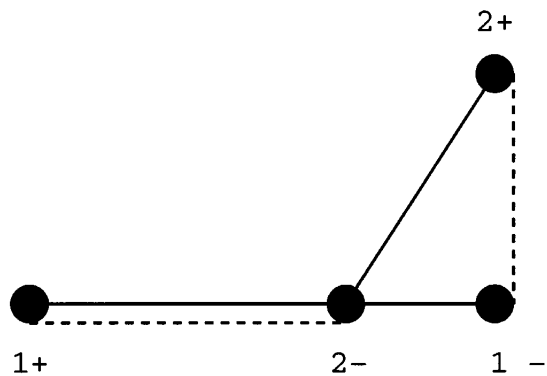


FIG. 7.—Same as in Figs. 4 and 5 for an idealized configuration of the loops in Fig. 6.

discussed in this section. Some comments are also made on the neglect of changes in the energy associated with the “potential” magnetic field.

4.1. Favorable Spot Configurations

Although the investigation of all the possible configurations of the spots in § 3 is far from complete, some favorable configurations are identified. An important qualitative point is that the mutual inductances play an important role in determining which configurations are favorable. For example, for collinear, overlapping loops of the same polarity (case 1a), the net self-inductance does not change during reconnection, and the energy change is due entirely to the mutual inductances.

Of the various configurations considered in § 3, the most favorable is the triangular configuration, that is, when a positive and a negative polarity footpoint are close together and one of the two final loops is small. This configuration is favorable over a wide range of angles from collinear ($\theta \sim 0$ in Fig. 4) to roughly orthogonal ($\theta \sim \pi/2$), but not when the initial loops are nearly collinear and antiparallel ($\theta \sim \pi$). It is instructive to consider why this final case ($\theta \sim \pi$ in Fig. 4) is relatively unfavorable. Simple intuition might incorrectly suggest that this is a favorable configuration because it allows a maximum reduction in the net self-inductance, due to reconnection forming two final loops with a net length substantially shorter than the net length of the initial loops. However, the mutual inductance between the initial loops is large and negative, implying that the initial magnetic energy is much less than would be (incorrectly) inferred by neglecting the mutual inductance. This is a general feature of reverse polarity configurations: these are unfavorable when the two initial loops are nearly antiparallel. However, a reverse polarity configuration is relatively favorable when the two initial loops are at a moderately large angle, so that the initial mutual inductance is small. Then there can be a reduction in the net self-inductance, which is not canceled by the change in the effective mutual inductance.

Another moderately favorable configuration is a square, with the initial loops along the diagonals. In this case the initial mutual inductance is zero, so that the initial magnetic energy is the sum of the two independent magnetic energies ($\frac{1}{2}L_1 I_1^2 + \frac{1}{2}L_2 I_2^2$). The reconnection causes a substantial reduction in the self-inductance: the self-inductance reduces by a factor $(1/2^{1/2})$ equal to the ratio of the length of sides to the diagonals of the square. However, the magnitudes of the

coefficients in equation (8) are smaller (by a factor ~ 2) than for the most favorable of the triangular configurations. This indicates that it is more favorable to have one of the final loops much shorter than the other (triangular case) than to have both of the comparable length (square case). This conclusion is also supported by consideration of the most favorable collinear configuration (case 1a), which is when the two initial loops (with the same polarity) are just touching so that the two final loops have $a_3 = a_1 + a_2$ and $a_4 = 0$.

The magnitudes of the coefficients in equation (8) can be, for the most favorable initial configurations, a significant fraction of the initial self-inductance. The coefficients can be written in the form $\mu_0 \Delta a$, where Δa is a characteristic length that is a substantial fraction of the radius of the smaller of the two initial loops, and where the parameter C in equation (9) is incorporated in the definition of Δa . For example, in the triangular case with initial loops of similar lengths $a_2 \sim a_1$ that are nearly orthogonal, the fraction is $\sim \frac{1}{3}(\Delta a \sim a_1/3)$.

4.2. The Energy Release in a Solar Flare

To be viable as a basis for interpreting solar flares, the model must account for the observed energy release in solar flares when the currents are of order those found observationally in flaring loops. The following estimates suggest that this requirement is satisfied.

Writing the coefficients in equation (8) in the form $\mu_0 \Delta a$, a length $\Delta a \sim 10^7$ m corresponds to a projected length $\sim 10''$ on the Sun. The loops involved in flares can have radii $\sim 10''$ or somewhat larger. This gives a characteristic value for the coefficients in equation (8) of $\mu_0 \Delta a \sim 10H$. Thus, for favorable configurations the coefficients in equation (8) can be of order several henry. A characteristic number for the energy available through reconnection in this model is then

$$\Delta E^{IR} \sim 10^{23} \left(\frac{\mu_0 \Delta a}{10H} \right) \left(\frac{\Delta I}{10^{11} \text{ A}} \right)^2 \text{ J.} \quad (26)$$

For example, for the five flares analyzed by Leka et al. (1996), the estimated currents ranged from $2\text{--}5 \times 10^{11}$ A. Assuming $\Delta I \sim 3 \times 10^{11}$ A, equation (26) implies a magnetic energy release of order 10^{24} J. Such an energy is adequate to account for the observed energy release in a moderately large flare.

An important requirement of the model is that both initial loops must be carrying a substantial current. The current ΔI in equation (26) is to be identified as the weaker of the two initial currents. With the resolution of presently available vector magnetograms, a loop with no detectable current would have $I \lesssim 10^{11}$ A. According to equation (26), the maximum energy that could be released in a flare in which the current in one loop is not detectable is $\sim 10^{23}$ J. One concludes that it is only for the most energetic flares that the currents in both initial loops should necessarily be detectable using existing techniques.

4.3. Observational Consequences of the Model

The present model can be tested in several ways. A direct quantitative test is to estimate the energy available and compare it with the energy observed to be released in a particular flare. The information required to calculate the energy available consists of (1) the locations of the spots

that form the footpoints of the reconnecting loops, and (2) the currents initially flowing in these loops. Then equation (8) gives the energy available, with the coefficients in equation (8) calculated as in the specific examples described in § 3.

In order to carry out such a comparison, one needs to identify the most favorable configurations for energy release in a systematic way and compare these with the spot configurations that lead to flares. From the cases considered in § 3, favorable configurations include two opposite polarity spots that are close together, so that one of the final loops is very short, and overlapping, nearly collinear loops forming a longer and a (nested) shorter loop. However, there are likely to be other configurations that may be more favorable, and these need to be identified before making any detailed comparison with observational data. As pointed out in § 3, a general configuration involves five free parameters. One of these may be regarded as a scaling parameter, leaving four free parameters to be optimized (subject to the constraint that the initial loops overlap) to find the most favorable shapes. Moreover, the cases $I_1 \gg I_2$, $I_1 = I_2$ and $I_2 \gg I_1$ in equation (8) need to be considered separately. Hence, a systematic search involves finding the maxima of three separate functions in a four dimensional space. A systematic investigation of parameter space to identify the most favorable configurations is being attempted.

Other ways in which the model might be tested relate to confirming that large currents are redirected from one flux loop to another as a result of reconnection during a flare. A direct signature of the current is the handedness or helicity, as discussed in § 5 below. The present model requires that any new flux loop formed during reconnection have the same handedness as the initial flux loops (cf. Berger & Field 1984), which also must both have the same handedness. One investigation of the helicity of active regions (Pevtsov, Canfield, & Medcalf 1995) found that the active regions that produce flares tend to have opposite to the generally prevailing helicity, but the statistical significance of this result is not high. It is not clear whether this result is in conflict with the model proposed here in that the important constraint in the model is that the reconnecting loops have the same helicity: several loops in an active region may have the same helicity whether or not this is opposite to the generally prevailing helicity. It might be remarked that the suggestion (Rust 1997) that helicity is conserved in space plasmas and that it has a characteristic sign in each solar hemisphere is consistent with the requirements of the present model. Although most of the observational evidence is consistent with Rust's hypothesis, the data on the helicity in flaring active regions (Pevtsov et al. 1995), which of most relevance here, is somewhat inconclusive concerning the sign of the helicity.

A less direct way of observing the currents is through the magnetic shear at the photosphere. Formation of a shorter loop, as if favored in the present model, implies that the current path moves closer to the photosphere. Qualitatively, formation of a shorter, current-carrying flux loop from a longer one, with the current conserved, should increase the shear at the photosphere. Such an increase, which is sometimes observed (e.g., Wang et al. 1994), is not expected in other models for flares.

4.4. Individual Reconnection Event

There is evidence for the energy release during the impul-

sive phases of solar flares occurring in discrete events with a range of timescales from milliseconds to tens of seconds (e.g., Sturrock et al. 1984; Benz 1987). In a reconnection model, such discrete events would correspond to discrete reconnection events, each such event involving a small value of $\Delta\Psi$ and ΔI . In the present model small individual reconnection events may be described by equation (4), with $I_{1f}, I_{2f}, I_{3i}, I_{4i}$ replaced by the instantaneous values of I_1, I_2, I_3, I_4 , respectively. The energy change associated with a discrete event involves the four coefficients M_n^{LCS} with $n = 1-4$ (cf. eq. [6]) but not the coefficient M^{IR} (cf. eq. [7]). In contrast, a single large flux transfer event (with ΔI the minimum of I_1 and I_2 here) involves only two coefficients M^{IR} and either M_1^{LCS} (for $I_1 > I_2$) or M_2^{LCS} (for $I_2 > I_1$). Thus, although it is assumed in the present paper that the condition for reconnection to occur is that $M^{\text{IR}} > 0$ and either $M_1^{\text{LCS}} > 0$ (for $I_1 > I_2$) or $M_2^{\text{LCS}} > 0$ (for $I_2 > I_1$), it is evident from these remarks on discrete reconnection events that the signs and magnitudes of the other coefficients are relevant to any modification of the present model to consider continuous reconnection. Although a detailed discussion of such discrete flux transfer events would be directly relevant to the interpretation of flare data, no such discussion is attempted in the present paper.

4.5. Formation of Large Loops by Multiple Reconnections

The existence of very long loops that connect different active regions has long been known from both radio data, specifically inverted-U radio bursts (e.g., Suzuki & Dulk 1985) and EUV and soft X-ray data, specifically from *Skylab* (e.g., Bray et al. 1991, p. 183). Their existence has been confirmed by more recent data (e.g., Tsuneta 1996; Mangharan et al. 1996). However, how such loops form is unclear. The discussion in § 3 (cases 1a and 2) of reconnection of overlapping collinear loops implies that it is energetically favorable for nearly aligned, current-carrying loops to reconnect to form larger loops. This suggests a possible explanation for how such loops might form. A very large loop can form by a sequence of reconnections, each of which increases the length of the loop only a moderate amount. For such large loops to form between two active regions requires that suitable small loops emerge in between active region, so that a sequence of reconnections could allow a loop to lengthen sequentially by reconnecting with many smaller loops until it spans the intervening region.

The observational data provide some support for the suggestion that long loops might form in this manner. Magnetic flux emerges from below the photosphere in the form of bipolar spots (e.g., the review by Zwaan 1985). Only roughly half the emerging magnetic flux is associated with large active regions. The flux that emerges between large active regions forms “ephemeral active regions” of which there are hundreds at any one time with a range of orientations and each with a lifetime ~ 1 hr (Harvey, Harvey, & Martin 1975). Ephemeral loops could allow sequential formation of a very long loop provided they have appropriate orientation and handedness. The range of orientations observed suggests that long loops could form in a variety of directions, and any preferred orientation would favor a long loop forming with this preferred orientation. As discussed in § 5 the requirement on the handedness should be satisfied. Thus, sequential reconnection with ephemeral loops appears to be a viable mechanism for forming long loops between active regions.

4.6. Neglect of Change in the Energy of the “Potential” Field

As stated in § 2.5, the change in the energy associated with “potential” field is ignored here, but the justification for this is weak. Another way of thinking about the change in magnetic energy associated with the “potential” field is in terms of currents confined to the corona.

The flux Ψ is not a true potential field: all models for coronal flux loops involve an implicit assumption concerning a surface current. The change in the energy of the “potential” field (eq. [11]) is actually a change in the energy associated with such localized currents, but the actual form of these currents is poorly understood. The requirement that the surface current be force free in the corona is a severe constraint. In particular, a cylindrical flux tube can have boundary conditions that require either $B_\phi = 0$ or $B_z = 0$ outside the flux tube, but both $B_\phi = 0$ and $B_z = 0$ simultaneously is not possible (e.g., Gold & Hoyle 1960; Melrose, Nicholls, & Broderick 1994). The boundary condition $B_z = 0$ outside the flux tube would be the more appropriate here, but would also be artificial. A more realistic model for a flux loop requires a more realistic boundary condition. Thus, the change in the energy associated with the “potential” magnetic field requires a realistic boundary condition that determines the form of the localized coronal currents and how they change during reconnection. No attempt is made to formulate such a model in the present paper.

The neglect of the change in energy associated with the “potential” magnetic field is based primarily on the evidence that flares correlate with regions of strong current flowing into and out of the corona. Any change in the “potential” field is related to currents that close entirely within the corona. A flare model based on energy release due to such currents is not excluded, and such a model would be an alternative to the model proposed here.

5. THE HANDEDNESS OF CORONAL MAGNETIC STRUCTURES

An important constraint implied by the reconnection model in § 2 is that reconnection is possible only between flux loops with the same handedness. The handedness is determined by the sign of I/Ψ , and both loops must have the same sign of this quantity so that current and flux can be transferred together during reconnection. Moreover, the handedness is related to the helicity, which is conserved during reconnection (Berger & Field 1984). In this section it is argued that the available observational data point strongly toward there being a preferred handedness for coronal flux loops.

It was pointed out by Martin, Marquette, & Bilimoria (1992) that there is a characteristic handedness to solar magnetic structures, and this has been discussed in more detail by Rust (1994, 1997), Rust & Kumar (1994, 1996), and Priest, van Ballegooijen, & MacKay (1996). The filaments are left hand (negative helicity) in the northern hemisphere and right hand (positive helicity) in the southern hemisphere (irrespective of the solar cycle). Pevtsov et al. (1995) considered the latitudinal variation of the photospheric magnetic helicity, based on a data set consisting of 69 diverse active regions. They found that 76% of the regions in the northern hemisphere had negative helicity and 69% of the regions in the southern hemisphere had positive heli-

city. They also found a tendency for active regions whose helicity does not obey the general rule, and whose helicity is time-variable, to produce more flares. Leka et al. (1996) found that the sense of twist of newly emerging bipoles is the same as the large-scale twist of the preexisting large spot ($I/\Psi < 0$). It might be noted that the suggestion that the observable twisting of flux loops is already present as they emerge had been made much earlier by Weart (1970, 1972), and also by Tanaka (1991), both of whom suggested that the ultimate seat of the activity is in the interior of the Sun where the twisted flux ropes are formed.

Seehafer (1990) considered the helicity of the electric current, defined by $\mathbf{B} \times (\nabla \times \mathbf{B})$. From a study of 16 active regions it was found that the electric current helicity is predominantly negative in the northern hemisphere and positive in the southern hemisphere. Seehafer (1990) noted that the sign of the electric current helicity produced by a standard α model for the solar dynamo is opposite to that observed. However, the sign is consistent with some alternative dynamo models, e.g., with that of Glatzmaier (1985). Rust (1996) has carried these arguments on magnetic helicity further to propose that helicity is conserved in space plasmas. Rust also noted that the correct handedness is produced by the Babcock model for the solar cycle, and also by Glatzmaier's (1985) model of the solar dynamo.

These various data on the handedness of magnetic structures and the sense of current flow are consistent with flux loops emerging with a characteristic sign of I/Ψ . Granted this, one would conclude that the requirement of the present model that the reconnecting flux tubes have the same sign of I/Ψ is normally satisfied. However, the most relevant data on active regions (Pevtsov et al. 1995) is inconclusive on this important point.

6. CONCLUSIONS

The model for solar flares proposed here is based on the assumption that the energy released in a flare is stored initially in currents that close deep in the solar atmosphere and that are already flowing in newly emerging flux loops. The energy release mechanism is assumed to be magnetic reconnection in which flux and current are transferred together between flux loops, subject to the constraints that the flux and current at each footpoint do not change during the reconnection process. In order for reconnection to occur the initial flux loops must be in contact, and the observational evidence suggests that this occur due to a rapid rise of emerging flux (Uchida et al. 1992). The loops are modeled as semi-tori with their axes in the photosphere, and the shapes of these tori are assumed fixed by the locations of the spots, so that they do not change during a flare. Thus, the semi-tori are actually shells of loops that may correspond to an actual loops or may be empty. A magnetic reconnection moves flux and current together between these shells, forming a new loop if one shell is initially empty, and destroying an initial loop if all its flux and current are transferred.

The conclusions from the present investigation can be summarized as follows:

1. The requirement for energy release is that the final

magnetic energy be less than the initial magnetic energy; the condition for this follows from equation (8) in the case where the maximum possible current is transferred.

2. Some favorable configurations for energy release are identified; these include two spots of opposite polarity being close together (so that one of the final loops is very short) and initial loops at a large angle to each other; if one of the flux loops has reverse polarity, reconnection is more favorable when the smaller loop has the strong current ($I_2 > I_1$ here). A systematic search of parameter space is required to identify other possible favorable configurations.

3. The magnitude of the energy release under favorable conditions depends on the current transferred, and for ΔI of a few 10^{11} A an energy release of a few 10^{24} J is possible; this is adequate to account for a moderately large flare.

4. The model requires that ΔI not exceed the smaller of the currents (I_1, I_2) in the initial loops, and the observable threshold for detection of a current from vector magnetograms is such that energy release up to about 10^{23} J would be compatible with currents below this present-day threshold of detectability.

5. Another favorable configuration for modest energy release is two overlapping collinear loops reconnecting to form a longer loop and a nested shorter loop; it is suggested that a sequence of such reconnections involving ephemeral flux loops might account for the formation of very long loops linking active regions.

6. The model requires that the reconnecting flux loops have the same handedness, defined by the sign of I/Ψ , which is also the sign of the helicity, and the helicity is conserved during reconnection. There is considerable evidence that coronal magnetic structures have a characteristic handedness, implying that this requirement is probable satisfied. However, there is also an indication (albeit with low statistical significance) that active region that produce flares have opposite to the prevailing helicity. Further observational data are required to clarify whether or not the observed helicities of reconnecting loops are consistent with the model.

7. The most direct observational test for the model is a comparison of the magnetic energy available for release with the energy actually released in a subsequent flare. The magnetic energy available can be calculated in terms of a known configuration of the spots and known currents in the initial loops. Other tests are that the helicity of a newly formed loop must be the same as that of the initial loops, and that, when a newly formed loop is smaller than the initial loops, the magnetic shear in the photosphere should increase as a result of the flare.

8. The energy associated with the "potential" field, described by the flux Ψ , should change during reconnection, and this change is ignored in the present model. Although it is argued that this neglect may be justified, the argument is a weak one. An alternative model for the energy release could be formulated based on the changes associated with the "potential" field.

I thank Lawrence Cram, Stephen Hardy, and Mark Walker for helpful comments on the manuscript.

APPENDIX

ESTIMATES OF THE MUTUAL INDUCTANCES

A simplifying assumption that allows the mutual inductance between two current loops to be evaluated is to replace the actual currents by line currents. Then one has

$$M_{nm} = \frac{\mu_0}{4\pi} \oint \oint \frac{d\ell_n \cdot d\ell_m}{r_{nm}}, \tag{A1}$$

where r_{nm} is the distance between the two line elements $d\ell_n$ and $d\ell_m$, and where $d\ell_n$ denotes an element of length around the path of the n th current loop. For two loop currents that have their axes aligned and their centers separated by a distance d_{nm} one has (e.g., Stratton 1941, p. 263; Batygin & Topytgin 1962, p. 254)

$$M_{nm} = \mu_0(a_n a_m)^{1/2} \left[\left(\frac{2}{k_{nm}} - k_{nm} \right) K(k_{nm}) - \frac{2}{k_{nm}} E(k_{nm}) \right], \quad k_{nm}^2 = \frac{4a_n a_m}{(a_n + a_m)^2 + d_{nm}^2}, \tag{A2}$$

where $K(k)$ and $E(k)$ are complete elliptic integrals (e.g., Abramowitz & Stegun 1965, p. 590). The leading term in the power series expansions,

$$K(k) = \frac{\pi}{2} \left(1 + \frac{k^2}{4} + \frac{9k^4}{64} + \dots \right), \quad E(k) = \frac{\pi}{2} \left(1 - \frac{k^2}{4} - \frac{3k^4}{64} - \dots \right), \tag{A3}$$

in equation (A2) reproduces the dipole approximation (see below). Two special cases treated by Jackson (1975, p. 263) are for two identical current loops, of radius a . For the case where their axes are aligned and are a distance d apart, Jackson quoted

$$M = \left[\left(\frac{a}{d} \right)^3 - 3 \left(\frac{a}{d} \right)^5 + \frac{75}{8} \left(\frac{a}{d} \right)^7 + \dots \right], \tag{A4}$$

where the expansion is for $d > 2a$. The result (eq. [A4]) is equivalent to equation (A2) for $a_n = a_m = a$, $d_{nm} = d$. For the case where the two loops are in the same plane, with the centers separated by a distance d , Jackson found

$$M = -\frac{\mu_0 \pi a}{4} \left[\left(\frac{a}{d} \right)^3 + \frac{9}{4} \left(\frac{a}{d} \right)^5 + \frac{375}{64} \left(\frac{a}{d} \right)^7 + \dots \right], \tag{A5}$$

for $d > 2a$.

For two loops whose axes intersect at an angle γ at a point where the radius a of one loop subtends an angle α and the radius b of the other loop subtends an angle β , the mutual inductance may be evaluated in terms of associated Legendre polynomials P_l^m (e.g., Gray 1972, pp. 5–31):

$$M = \pi \mu_0 b \sin \alpha \sin \beta \sum_{l=1}^{\infty} \frac{\sin \alpha \sin \beta}{l(l+1)} \left(\frac{b}{a} \right)^l P_l^1(\cos \alpha) P_l^1(\cos \beta) P_l(\cos \gamma). \tag{A6}$$

In the limit $b \ll a$ only the term $l = 1$ need be retained, and then equation (A6) gives $M \approx \pi \mu_0 (b^2/2a) \sin^2 \alpha \sin^2 \beta \cos \gamma$. Furthermore, for loops aligned along their axes, one has $\gamma = 0$, $\sin \beta = 1$ and $\sin \alpha = a/(a^2 + d^2)^{1/2}$, where d is the separation between their centers.

One case not covered by the foregoing standard results is the case of nearby loops at an oblique angle to each other. Consider the particular case of two loops with a common center, with radii a and b , and at an angle θ to each other. The integral (A1) gives

$$M(\theta) = \frac{\mu_0 ab}{4\pi} \int_0^{2\pi} d\phi_1 \int_0^{2\pi} d\phi_2 \frac{\cos \theta \cos \phi_1 \cos \phi_2 + \sin \phi_1 \sin \phi_2}{[a^2 + b^2 - 2ab(\cos \phi_1 \cos \phi_2 + \cos \theta \sin \phi_1 \sin \phi_2)]^{1/2}}. \tag{A7}$$

For arbitrary θ the integral in equation (A7) may be evaluated approximately for $b \ll a$ by expanding in powers of b/a . The leading term gives

$$M(\theta) = \frac{\mu_0 \pi b^2 \cos \theta}{2a}. \tag{A8}$$

The result (eq. [A8]) is similar to the approximate forms mentioned following equation (A6). The interpolation (10) includes these cases when one loop is much smaller than the other.

If the distances between the current loops is sufficiently large (compared with the sizes of the loops), the magnetic dipole approximation applies. The mutual inductance of two magnetic dipoles, \mathbf{m}_n and \mathbf{m}_m , whose centers are separated by a distance $d_{nm} = |\mathbf{x}_{nm}|$, where \mathbf{x}_{nm} is the vector displacement between them, is

$$M_{nm} = -\frac{\mu_0 \pi a_n^2 a_m^2}{4d_{nm}^3} \left(\mathbf{n}_n \cdot \mathbf{n}_m - \frac{3\mathbf{n}_n \cdot \mathbf{x}_{nm} \mathbf{n}_m \cdot \mathbf{x}_{nm}}{d_{nm}^2} \right). \tag{A9}$$

In the case where the magnetic dipoles are aligned along the line joining them ($\mathbf{n}_n, \mathbf{n}_m, \mathbf{x}_{nm}$ all parallel) equation (A9) reproduces the leading term in the result obtained from equation (A2) in the limit $k_{nm} \ll 1$ using equation (A3), which reduces to the leading term in equation (A4) for $a_n = a_m = a$ and $d_{nm} = d$. Also for $\mathbf{n}_n, \mathbf{n}_m$ parallel and orthogonal to \mathbf{x}_{nm} , (eq. [A9]) reproduces the leading term in equation (A5) for $a_n = a_m = a$ and $d_{nm} = d$. The interpolation formula (10) gives the correct

dipole dependence $\propto 1/d_{nm}^3$ for large d_{nm} , and although it does not reproduce the correct angular dependence in the dipole approximation in general (cf. eq. [A9]), it is correct in the special case where one of the dipoles is aligned with the line joining their centers.

REFERENCES

- Abramowitz, M., & Stegun, I. A. 1965, *Handbook of Mathematical Functions* (New York: Dover)
- Alfvén, H., & Carlqvist, P. 1967, *Sol. Phys.*, 1, 220
- Bagalá, L. G., Mandrini, C. H., Rovira, M. G., Démoulin, P., & Hénoux, J. C. 1995, *Sol. Phys.*, 161, 103
- Batygyn, V. V., & Toptygin, I. N. 1962, *Problems in Electrodynamics* (New York: Academic Press)
- Baum, P. J., & Bratenahl, A. 1980, *Sol. Phys.*, 67, 245
- Benz, A. O. 1987, *ApJ*, 211, 270
- Berger, M. A., & Field, G. B. 1984, *J. Fluid Mech.*, 147, 133
- Book, D. L., Turchi, P. J., & Stein, D. L. 1979, *J. Comp. Phys.*, 33, 271
- Bray, R. J., Cram, L. E., Durrant, C. J., & Loughhead, R. E. 1991, *Plasma Loops in the Solar Corona* (Cambridge: Cambridge Univ. Press)
- Brown, J. C., et al. 1994, *Sol. Phys.*, 153, 19
- Démoulin, P., Bagalá, L. G., Mandrini, C. H., Hénoux, J. C., & Rovira, M. G. 1997, *A&A*, submitted
- Démoulin, P., Hénoux, J. C., & Mandrini, C. H. 1994, *A&A*, 285, 1023
- Démoulin, P., van Driel-Gesztelyi, L., Schmieder, B., Hénoux, J. C., Csepura, G., & Hagyard, M. J. 1993, *A&A*, 271, 292
- Gary, G. A., & Démoulin, P. 1995, *ApJ*, 445, 982
- Glatzmaier, G. A. 1985, *ApJ*, 291, 300
- Gold, T., & Hoyle, F. 1960, *MNRAS*, 120, 89
- Gorbachev, V. S., & Somov, B. V. 1988, *Sol. Phys.*, 150, 77
- . 1989, *Sov. Astron. AJ*, 33, 57
- Gray, D. E. 1972, *American Institute of Physics Handbook* (Third ed.; New York: McGraw-Hill)
- Harvey, K. L., Harvey, J. W., & Martin, S. F. 1975, *Sol. Phys.*, 40, 87
- Heyvaerts, J., Priest, E. R., & Rust, D. M. 1977, *ApJ*, 216, 123
- Jackson, J. D. 1975, *Classical Electrodynamics* (New York: Wiley)
- Landau, L. D., & Lifshitz, E. M. 1960, *Electrodynamics of Continuous Media* (Oxford: Pergamon)
- Leka, K. D., Canfield, R. C., McClymont, A. N., & van Driel-Gesztelyi, L. 1996, *ApJ*, 462, 547
- Longcope, D. W. 1996, *Sol. Phys.*, 169, 91
- Machado, M. E., Moore, R. L., Hernandez, A. M., Rovira, M. G., Hagyard, M. J., & Smith, J. B., Jr. 1988, *ApJ*, 326, 425
- Mandrini, C. H., Démoulin, P., Hénoux, J. C., & Machado, M. E. 1991, *A&A*, 250, 541
- Mandrini, C. H., Démoulin, P., Rovira, M. G., de la Beaujardière, J.-F., & Hénoux, J. C. 1995, *A&A*, 303, 927
- Mandrini, C. H., Rovira, M. G., Démoulin, P., Hénoux, J. C., Machado, M. E., & Wilkinson, L. K. 1993, *A&A*, 272, 609
- Mangharan, P. K., van Driel-Gesztelyi, L., Pick, M., & Démoulin, P. 1996, *ApJ*, 468, L73
- Martin, S. F., Marquette, W. H., & Bilimoria, R. 1992, in *ASP Conf. 27, Solar Cycle*, ed. K. L. Harvey (San Francisco: ASP), 53
- Melrose, D. B. 1991, *ApJ*, 381, 306
- . 1992, *ApJ*, 387, 403
- Melrose, D. B., Nicholls, J., & Broderick, N. G. 1994, *J. Plasma Phys.*, 51, 163
- Nishio, M., Yaji, K., Kosugi, T., Nakajima, H., & Sakurai, T. 1997, *ApJ*, submitted
- Pevtsov, A. A., Canfield, R. C., & Metcalf, T. R. 1995, *ApJ*, 440, L109
- Priest, E. R., van Ballegoijen, A., & MacKay, D. H. 1996, *ApJ*, 460, 530
- Rust, D. M. 1994, *Geophys. Res. Lett.*, 21, 241
- . 1997, in *Coronal Mass Ejections: Causes and Consequences*, ed. N. Crooker, J. Joselyn, & J. Feynman (AGU Geophysical Monograph Series), in press
- Rust, D. M., & Kumar, A. 1994, *Sol. Phys.*, 150, 69
- . 1996, *ApJ*, 464, L199
- Seehafer, N. 1990, *Sol. Phys.*, 125, 219
- Stratton, J. A. 1941, *Electromagnetic Theory* (New York: McGraw-Hill)
- Sturrock, P. A., Kaufmann, P., Moore, R. L., & Smith, D. F. 1984, *Sol. Phys.*, 94, 341
- Suzuki, S., & Dulk, G. A. 1985, in *Solar Radiophysics*, ed. D. J. McLean & N. R. Labrum (Cambridge: Cambridge Univ. Press), 322
- Švestka, Z. 1976, *Solar Flares* (Dordrecht: Reidel)
- Sweet, P. A. 1958, *Nuovo Cimento Suppl.*, 8, 188
- Tanaka, K. 1991, *Sol. Phys.*, 136, 133
- Tsuneta, S. 1996, *ApJ*, 456, L63
- Uchida, Y., McAllister, A., Strong, K. T., Ogawara, Y., Shimizu, T., Matsu-moto, R., & Hudson, H. S. 1992, *PASJ*, 44, L155
- Van Driel-Gesztelyi, L., Hofmann, A., Démoulin, P., Schmieder, B., & Csepura, G. 1994, *Sol. Phys.*, 149, 309
- Wang, H., Ewell, M. W., Zirin, H., & Ai, G. 1994, *ApJ*, 424, 436
- Wang, T., Xu, A., & Zhang, H. 1994, *Sol. Phys.*, 155, 99
- Weart, S. R. 1970, *ApJ*, 162, 987
- . 1972, *ApJ*, 177, 271
- Zirin, H., & Liggett, M. A. 1987, *Sol. Phys.*, 113, 267
- Zwaan, C. 1985, *Sol. Phys.*, 100, 397